1

Hardening and Softening in Magnesium Alloys

Pavel Lukáč and Zuzanka Trojanová,
Charles University in Prague,
Czech Republic

1. Introduction

There is an increasing interest in automobile and aerospace industries for lightweight materials (alloys and metal matrix composites). Magnesium alloys with their high specific strength (the strength-to-density ratio – σ/ρ) may be used as structural materials. Over the last two decades, use of magnesium alloys has progressively grown. Different magnesium alloys have been developed and tested. Research and development of magnesium alloys have shown that they have a great potential for applications as the lightweight materials. This is because of their high specific strength, high damping capacity and good machinability. However, their applications are limited at elevated temperatures. New alloys with improved creep resistance and high strength have been developed in recent years. Among the alloys, the Mg-Al-Ca and Mg-Al-Sr alloys exhibit good creep resistance due to the presence of thermally stable phases. During plastic deformation over wide ranges of temperature and strain rate, different micro-mechanisms may play important role. It is important to estimate the mechanisms responsible for the deformation behaviour – hardening and softening – of the alloys. An analysis of deformation microstructures has shown that one should consider dislocation-based mechanisms in order to explain the deformation behaviour. The values of strength may be influenced by different hardening mechanisms.
The aim of this paper is to present the deformation behaviour of some magnesium alloys at different temperatures and to propose the mechanisms responsible for plastic deformation of the alloys.

2. Stress strain curves

A set of the true stress – true strain curves for some magnesium alloys deformed in tension or in compression at different temperatures are shown in Figs. 1-3. It can be seen that the shape of the deformation curves depends very sensitively on the testing temperature. At lower temperatures (lower than about 150 °C), the flow stress increases with strain – a high strain hardening is observed. On the other hand, at temperatures higher than 200 °C, the stress – strain curves are flat; the strain hardening rate is close to zero. It means there is a dynamic balance between hardening and softening; hardening is compensated for by recovery. Strain hardening – the change in the flow stress with strain – depends on the dislocation structure evolved with plastic deformation. An increase in the flow stress is due to dislocation storage. Dislocations stored at obstacles contribute to hardening, whereas cross slip and/or climb of dislocations contribute to softening. Dislocations after cross slip

or after climb may annihilate, the dislocation density decreases, which causes a decrease of the flow stress with strain, i.e. a decrease in the strain hardening rate. Interplay between work hardening and softening may help to account for the deformation behaviour. In the following we shall present some models describing the stress dependence of the strain hardening rate in metallic materials.

3. Strain hardening models

It is widely accepted that the resolved shear stress, τ, necessary for the dislocation motion in the slip plane can be divided into two components:

$$\tau = \tau_i + \tau^*, \tag{1}$$

where τ_i is the internal stress and $\tau^*$is the thermal component, oft called effective stress. The effective stress acts on dislocations during their thermally activated motion when they overcome short range obstacles as forest dislocations, solute atoms, etc. The internal stress component can be expressed as

$$\tau_i = \alpha_1 G b \rho_t^{1/2}, \tag{2}$$

where ρ_t is the total dislocation density, G is the shear modulus, b is the magnitude of the Burgers vector and α_1 is a constant.
The applied stress σ acting on a polycrystal is related to the resolved shear stress τ by the Taylor factor M:

$$\sigma = M \tau. \tag{2}$$

Then similarly σ may be also divided into the internal and effective stress components

$$\sigma = \sigma_i + \sigma^* \tag{3}$$

Stress relaxation can be considered as a method for studying the internal stress field, based on the separation of the flow stress, i. e. on the determination of the average effective internal stress $(\sigma_i)_{eff}$. For the simplicity it will be called the internal stress σ_i.
In spite of very long time investigating of polycrystals up to now, the generally accepted analytical description of the stress - strain curves does not exist. It is a consequence of the complicated nature of the stress in polycrystals, which is dependent on many structure parameters as type of crystal structure, grain size, texture, concentration and distribution of solute atoms, presence of second phase, etc. A change of the flow stress is connected with development of the material structure. This development depends on strain, temperature, strain rate, preceding history of the sample, and on other parameters. Up to now it was not detailed investigated. It is considered, for simplicity, that the plastic deformation is determined by one main structural parameter S that describes the actual structural state of the material.
The flow stress of crystalline materials σ depends on the dislocation structure and is related to the dislocation density, ρ, as

$$\sigma = \alpha_1 M G b \rho^{1/2}, \tag{4}$$

where G is the shear modulus, b is the magnitude of the Burgers vector. The relationship (4) implies that the strength of the material is determined by dislocation-dislocation interaction.

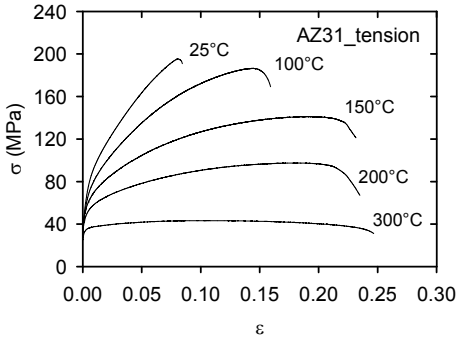

Fig. 1. Stress strain curves obtained for AZ31 gravity cast alloy at various temperatures in tension.

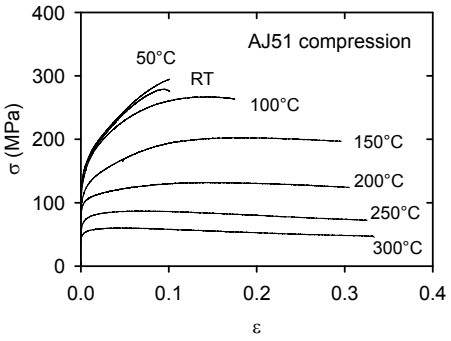

Fig. 2. Stress strain curves obtained for AJ51 squeeze cast alloy at various temperatures in compression.

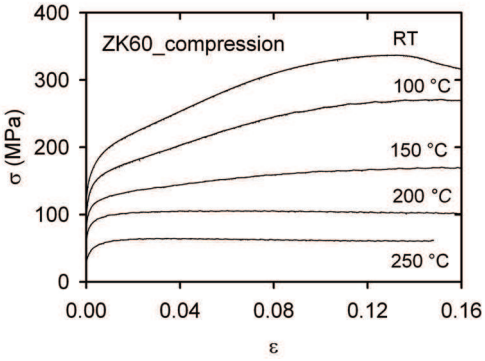

Fig. 3. Stress strain curves obtained for ZK60 alloy deformed in compression at various temperatures.

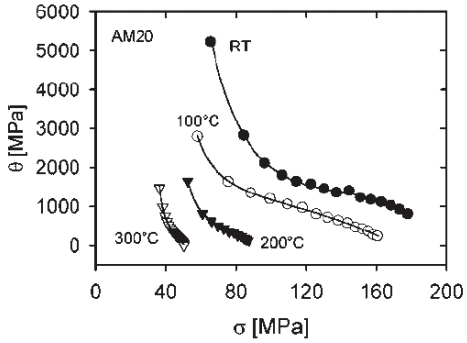

Fig. 4. Work hardening coefficient versus stress obtained for AM20 alloy deformed in tension at various temperatures.

The evolution equation describing the development of the dislocation structure with time or strain can be generally described in the following form:

$$\frac{d\rho}{d\varepsilon} = \left(\frac{d\rho}{d\varepsilon}\right)_h - \left(\frac{d\rho}{d\varepsilon}\right)_r . \tag{5}$$

The first (positive) term on the right hand accounts for the dislocation storage, while the second one represents the annihilation of dislocations; it contributes to softening.

Model of Kocks

Kocks (Kocks, 1976) has assumed that the dislocation mean free path is proportional to the average spacing between forest dislocations. He considered that an increase in the dislocation density with strain is due to dislocation storage and a decrease in the dislocation density is caused by annihilation of dislocations by cross slip.
Then, the evolution equation for the dislocation density reads:

$$\frac{d\rho}{d\varepsilon} = \kappa_f \rho^{1/2} - \frac{L_r \rho}{b}, \tag{6}$$

where L_r is the average length of the dislocation segment recovered in one recovery event (due to cross slip), κ_f is a geometrical factor based on the assumption that the mean free path Λ of the dislocation glide is proportional to the average spacing between forest dislocations ℓ_d i.e.

$$\Lambda = \beta \ell_d = \beta \rho^{-1/2}. \tag{7}$$

L_r is a function of temperature and strain rate. The stress dependence of the strain hardening rate of polycrystals (it is necessary to take into account the relationship between work hardening coefficient (rate) of single crystals and polycrystals) $\Theta = d\sigma / d\varepsilon = M^2\theta$, ($\sigma = M\tau$, $\varepsilon = \gamma/M$, $\theta = d\tau/d\gamma$).can be written.

$$\Theta = \frac{d\sigma}{d\varepsilon} = \Theta_{0K}\left(1 - \frac{\sigma}{\sigma_{SK}}\right), \tag{8}$$

where $\Theta_{0K} = \dfrac{\alpha_1 M^2 G b \kappa_f}{2}$ and $\sigma_{SK} = \dfrac{\alpha_1 M G b^2 \kappa_f}{L_r}$.

In many cases, equation (8) cannot describe the whole work hardening curve that consists of several regions with different slopes. This phenomenon is common for many materials. It should be mentioned that texture influences the hardening parameters and therefore, variation in M can be large (Cáceres & Lukáč, 2008).

Model of Estrin and Mecking

In contrary to the model of Kocks, Estrin and Mecking (Estrin & Mecking, 1984) have assumed that the mean free path of dislocations Λ is constant and it is determined by the spacing between impenetrable obstacles (grain boundaries, incoherent precipitates, dispersion particles). Finally they obtained

$$\frac{d\rho}{d\varepsilon} = \frac{1}{bs} - \frac{L_r}{b}\rho \tag{9}$$

and

$$\sigma\Theta = \Theta_{0EM}\left(1 - \frac{\sigma^2}{\sigma_{SEM}^2}\right), \tag{10}$$

where $\Theta_{0EM} = \dfrac{M^3(\alpha_1 G b)^2}{2sb}$, $\sigma_{SEM} = \dfrac{M\alpha_1 G b}{\left(sL_r\right)^{1/2}}$ and s is the particle spacing or the grain size.

Model of Malygin

Malygin (Malygin, 1990) took into account: storage of dislocations on impenetrable obstacles, storage of dislocations on forest dislocations and annihilation of dislocations due to cross slip. The evolution equation has, in this case, the following form:

$$\frac{d\rho}{d\varepsilon} = \frac{1}{bs} + \kappa_f \rho^{1/2} - \kappa_a \rho, \tag{11}$$

where s is the particle spacing or the grain size, κ_f is the coefficient of the dislocation multiplication intensity due to interaction of moving dislocations with forest dislocations and κ_a is the coefficient of the dislocation annihilation intensity due to cross slip. Finally, the equation suitable for an analysis of the experimental strain hardening rate of polycrystals is then

$$\Theta = d\sigma / d\varepsilon = \mathcal{A}/ (\sigma - \sigma_y) + \mathcal{B} - C(\sigma - \sigma_y). \quad (12)$$

Here the following substitutions were made:

$$\mathrm{A} = \frac{1}{2} M^3 (\alpha_1 G b)^2 \frac{1}{bs};\ \mathrm{B} = \frac{1}{2} M^2 \alpha_1 G b \kappa_f;\ \text{and } \mathrm{C} = \frac{1}{2} M \kappa_a .$$

The yield stress σ_y corresponds to the beginning of plastic deformation and comprises all contributions from the various hardening mechanisms.

The model of Lukáč and Balík

In many cases, the Malygin model describes the whole work hardening curve at lower temperatures where only stage II and III hardening occurs. At intermediate temperatures (about 0.3 T_m), there are deviations from the prediction of this model, which indicates the presence of some other recovery process in addition to cross slip. Lukáč and Balík (Lukáč & Balík, 1994) assumed that hardening occurs due to multiplication of dislocations at both non-dislocation obstacles and forest dislocations. As the dominant softening processes, annihilation of dislocations due to both cross slip and climb are considered. They derived the kinetic equation for single crystals in the following form:

$$\frac{d\rho}{d\gamma} = \frac{1}{bs} + \kappa_f \rho^{1/2} - \frac{cL_{CS}}{b} - \frac{D_c b^2 \psi_c}{\chi k_B T \dot{\gamma}} \tau \rho^{3/2}, \quad (13)$$

where L_{CS} is the dislocation segment length recovered by one cross slip event, c is the area concentration of the recovery sites in a slip plane, ψ_c is a fraction of the dislocations which can be annihilated by climb of dislocations with jogs, χ is a parameter which gives the relation between dislocation climb distance w (i.e. distance between storage of a dislocation and its annihilation site) and the average dislocation spacing $1/\sqrt{\rho}$ in the form $w = \chi / \sqrt{\rho}$, τ is the shear stress, γ is the shear strain, k_B is the Bolzmann constant and D_c is an abbreviation which includes the diffusion coefficient and the stacking fault energy. The stress dependence of the work hardening rate for polycrystals reads:

$$\Theta = A/(\sigma - \sigma_y) + B - C(\sigma - \sigma_y) - D(\sigma - \sigma_y)^3 . \quad (14)$$

Here the meaning of the parameters used is the following:

$$A = M^3 (\alpha_1 G)^2 \frac{b}{2s} \left(\frac{\dot{\varepsilon}}{\dot{\varepsilon}_1} \right)^{\frac{2}{n}};\ B = \frac{1}{2} M^2 \alpha_1 G n \kappa_f \left(\frac{\dot{\varepsilon}}{\dot{\varepsilon}_1} \right)^{\frac{1}{n}};\ C = M \frac{cL_{CS}}{2b\rho};\ D = \frac{1}{M^2} \frac{\psi_c D_c b}{2\chi \alpha_1 G k_B T \dot{\varepsilon}} \left(\frac{\dot{\varepsilon}}{\dot{\varepsilon}_1} \right)^{-\frac{1}{n}}$$

Here $\dot{\varepsilon}_1$ is a parameter and n is the stress exponent. It should be mention that, in the face-centred-cubic metals, the parameters A and B are independent of temperature and the parameters C and D depend on temperature.

Model of Estrin and Kubin.

In many cases, a model employing just one internal variable (the total dislocation density) is not sufficient for describing deformation histories involving rapid changes of the deformation path. Instead of using a single internal variable related to the total dislocation density ρ, Estrin and Kubin (Estrin & Kubin, 1986) considered the density of mobile dislocation ρ_m and the relatively immobile dislocation density (or the forest dislocation density) ρ_f. The evolution equations for the two populations of dislocations proposed by Estrin and Kubin can be expressed as

$$\frac{d\rho_m}{d\gamma} = -k_1\sqrt{\rho_f} - k_3\rho_m + k_4\frac{\rho_f}{\rho_m} \tag{15}$$

$$\frac{d\rho_f}{d\gamma} = k_1\sqrt{\rho_f} - k_2\rho_f + k_3\rho_m . \tag{16}$$

Here k_i are constants. It can be seen that the negative terms in Eq. (15), which represent the loss of the mobile dislocation density due to various dislocations reaction, reappear as positive terms in eq. (16). Newly formulated two variable constitutive model was solved by Estrin (Estrin, 1996) and Braasch, Estrin and Brechet (Braasch et al., 1996).

Model of Nes

Three parameters approach to the modelling of metal plasticity has been proposed by Nes & Marthinsen (Nes & Marthinsen, 2002). It is assumed in the model that at small strains (stage II) the stored dislocations are arranged in a cell structure which may be characterised by thickness t of cell walls; internal dislocation density ρ_b; dislocation density within cells. At large strains (stage IV), the cell walls collapse into sub-boundaries with a misorientation φ. The main features of the model can be summarised as follows:

1. The flow stress τ is done by

$$\tau = \tau_i + \alpha_1 Gb\sqrt{\rho_i} + \alpha_2 Gb/\delta , \tag{17}$$

where τ_I is the frictional stress, α_1 and α_2 are constants, and δ is the size of cells or subgrains. The frictional stress reflects short range interactions associated with the intersection of forest dislocations and dragging of jogs which can be expressed by

$$2\sinh\frac{\tau_i V_a}{k_B T} = \left(b^2\rho_m C_i \nu_D\right)^{-1}\dot{\gamma}\exp\left(\frac{U_i}{k_B T}\right), \tag{18}$$

where V_a is the activation volume, U_i is the activation energy, ρ_m is the mobile dislocation density ν_D the Debye frequency and C_i is a constant; k_B T has its usual meaning.

2. Dislocations are stored during deformation in three sites: in the cell interior, in old boundaries and/or by forming new boundaries. These processes can be described by the following equation

$$\frac{d\rho_{nb}^{+}}{d\gamma} = 2S\rho_i \frac{L}{b}, \tag{19}$$

where ρ_{nb} are dislocations stored in new boundaries, L is the mean free path of dislocations before being stored, $L=C\rho^{-1/2}$ (C is a constant), ρ is the total density of stored dislocations. S is dislocation storage parameter that can be defined using microstructural scaling C_i constants and volume fraction of cell walls f: $S=S_{sc}=S_{sc}(f, C_c, C_t, C_{cb})$, where $C_c=\delta\rho_i^{1/2}$, $C_t=t/\delta$ and $C_{cb}=\delta\rho_b^{1/2}$. Equation (19) can be expressed in the following alternative forms:

Stage II: $\frac{d\rho_i^{+}}{d\gamma} = -\frac{2\rho_i^{1/2}}{bC\left[1-f+\left(C_b/C_c\right)^2\right]^{1/2}}$

Stage III and IV: $\frac{d\delta^{-}}{d\gamma} = -\frac{2\rho_{III}SC\delta^2}{\kappa\varphi\left(\rho_{III}+\kappa\varphi/b\delta\right)^{1/2}}$

where $C_b=fC_{cb}$ and κ is a geometric constant that is equal to 2 for a regular cell structure. Based on experimental observations the sub-boundary orientation, φ, depends on δ in stage III and becomes a constant in stage IV, while S is treated as a modelling parameter.

3. Dynamic recovery is incorporated assuming two mechanisms: a) a dislocation segment in a Frank network which may migrate under a force per unit length, F, with a velocity

$$\upsilon = \upsilon_D b C_\rho^{1/2} \exp\left(-\frac{U_\rho}{kT}\right) 2\sinh\frac{Fb^2}{k_B T},$$

where $F=\alpha_3\xi_\rho Gb^2\rho_i^{1/2}$, C_ρ and α_3 are constants, U_ρ is the activation energy and ξ_ρ a dynamic stress intensity factor. The average subgrain size will increase according to

$$\frac{d\delta^{+}}{dt} = \dot{\gamma}\frac{d\delta^{+}}{dt} = \upsilon_D b C_\delta \rho^{1/2} \exp\left(-\frac{U_\delta}{k_B T}\right) 2\sinh\frac{pV_a}{k_B T},$$

where V_a is the activation volume. It should be mentioned that the models mentioned above were developed for polycrystals of face-centred-cubic metals that have more than 5 independent slip systems. On the other hand, hexagonal metals with the low symmetry do not provide 5 identical slip systems. To fulfil the von Mises criterion for polycrystal deformation, several different crystallographic slip systems have to be activated.

In magnesium and its alloys, the dominant slip mode is the basal slip with two independent modes, which is not sufficient for the satisfying the von Mises criterion. The glide of dislocation in second-order pyramidal slip systems should be considered.

Comparison with experimental results

Comparing experimental stress strain curves (for example curves introduced in Figs. 1-3) with the models of the strain hardening, the best agreement for hexagonal magnesium alloys was found for the Lukáč and Balík model (L-B model). Corresponding stress dependences of the work hardening coefficients are introduced in Fig. 4. From Fig. 4 it can be easily seen that the work hardening coefficient Θ does not decreases with the increasing stress linearly; then the Kocks model may not work. Note that the Nes model was not analysed because of missing dislocation substructure data. Parameters following from the L-B model are introduced in Table 1 (Máthis & Trojanová, 2005).

	A (MPa^2)	B (MPa)	C	D x 10^4 (MPa^{-2})	R^2	σ_y (MPa)	σ_{02} (exp) (MPa)
0.2%Zn	820 ± 178	2010 ± 20	5.4 ± 0.3	2.77 ± 0.07	0.987	57.40 ± 0.10	59
0.3%Zn	930 ± 60	1750 ± 10	0.5 ± 0.2	4.97 ± 0.05	0.988	71.48 ± 0.07	71
0.4%Zn	1940 ± 160	1910 ± 20	4.2 ± 0.3	2.30 ± 0.04	0.986	65.76 ± 0.04	70
1%Zn	1870 ± 170	1780 ± 20	2.7 ± 0.3	1.65 ± 0.06	0.97	87.28 ± 0.06	86
2%Zn	11100 ± 600	1780 ± 30	1.6 ± 0.3	1.00 ± 0.04	0.984	97.80 ± 0.20	100
3%Zn	46000 ± 6000	1360 ± 190	3e-3 ± 1.7	1.17 ± 0.28	0.988	114.70 ± 0.10	109

Table 1. Concentration dependence of the parameters of best fit for the L-B model and the calculated and measured yield stress for Mg-Zn alloys.

	A (MPa^2)	B (MPa)	C	D x 10^4 (MPa^{-2})	R^2	σ_y (MPa)	σ_{02} (exp) (MPa)
20 °C	68.700 ± 400	1532 ± 12	0	3.5 ± 0.6	0.99	78.3 ± 0.2	79
50 °C	49.200 ± 600	1471 ± 23	0	2.5 ± 0.7	0.99	61.2 ± 0.2	68
100 °C	54.800 ± 400	846 ± 15	0	4.4 ± 0.1	0.99	67.0 ± 0.7	69
150 °C	29.000 ± 100	346 ± 29	0	9.3 ± 0.1	0.99	67.0 ± 0.3	65
200 °C	4.173 ± 896	691 ± 52	14.1 ± 0.6	6.0 ± 0.3	0.97	64.2 ± 0.2	64

Table 2. Temperature dependence of the parameters of best fit to L-B-model and the calculated and measured yield stress for Mg alloy AM60.

The parameter A increases monotonically with the increasing solute content for Mg-Zn alloys in agreement with the prediction of the model, i.e. the parameter A is reciprocally proportional to the distance of impenetrable obstacles. The results suggest the increasing role of non-dislocation obstacles (e.g. solute atoms, clusters, precipitates, dispersoids) in the hardening mechanism. The parameter B remains nearly constant for all concentrations. Since this parameter is connected with the dislocation – forest dislocation interaction, this result indicates that the dislocation density in non-basal slip systems does not change with increasing solute content. There is a significant difference in parameter C, which characterizes the cross slip of screw dislocations. Cross slip takes place through prismatic slip system, and an increased activity of this slip system could enhance the ductility. In the case of Mg-Zn alloys, values of parameter C are of the order assumed by the model and

suggest the importance of cross slip in the deformation process. The concentration dependencies of this parameter (see Table 1) and ductility are in agreement, i.e. decrease with increasing concentration of Zn, thus the probability of cross slip decreases as well. It seems that 2 at.% Zn is a critical concentration; above that Zn content ceases improving the slip in prismatic slip system. It is necessary to remark that the model is able to describe drop in ductility for 0.3 at.% Zn, where the value of parameter C is small. This result supports the hypothesis of Akthar and Tegthsoonian (Akthar & Tegthsoonian, 1972), who assumed a hardening in prismatic plane for this concentration of Zn. Decreasing of parameter D with increasing solute content is most probably connected with reduced climb ability because of the high concentration of solute atoms along the dislocation line, and due to the lowering of the stacking fault energy as the solute content increases. Lowering of stacking fault energy improves the twinning activity as well. Note that the twin boundaries may be the impenetrable obstacles for dislocation motion. In materials with the strong texture (rolled sheets) when twinning is unfavourable it is necessary to consider the evolution of the dislocation substructure in both basal and non-basal slip systems, as it was shown by Balík et al. (Balík et al., 2009).

Similar analysis according to L-B model was performed for magnesium alloy AM60 deformed at various temperatures by Máthis et al. (Máthis et al., 2004a) Results are introduced in Table 2. The parameter A is not expected to depend on temperature, while Table 2 shows that the value of A drops rapidly above 150 °C. Alloy AM60 contains about 4% volume fraction of the intermetallic phase $Mg_{17}Al_{12}$, which is likely to dissolve as the temperature is increased. This will result in increased spacing between non-dislocations obstacles, which, in turn, would lower the value of the parameter A. Similarly, a decrease in the forest dislocation density (the density of dislocations in non-basal planes) can be expected at increasing temperatures. The mean free path of dislocations and therefore the storage distance will increase. The storage probability should decrease. This could cause the temperature decrease in the parameter B. The parameter C becomes >0 at 200 °C, which indicates that the cross slip becomes a significant recovery process at higher temperatures. The parameter D increases with increasing temperature, which is expected in the case of climb. Above 250 °C the model does not describe the experimental curves satisfactory; we suggest that another softening mechanism, most likely dynamic recrystallisation, may become operative.

4. Internal stress in magnesium alloys

In the stress relaxation tests, specimen is deformed to a certain stress (strain) and then allowed to relax by stopping the machine. Stress relaxation (SR) is usually analysed under an assumption that the strain rate during the SR experiments is proportional to the stress rate (the stress drops in one second). Components of the applied stress (σ_i, σ^*) can be estimated using Li's method (Li, 1967, 1981). The SR curves were fitted to a power law function in the form:

$$\sigma - \sigma_i = \left[a(m-1)\right]^{\frac{1}{1-m}} \left(t + t_0\right)^{\frac{1}{1-m}}, \tag{20}$$

where a, t_0, and m are fitting parameters.

A part of the AX41 true stress – true strain curve measured in compression at 25 °C with points indicating the stresses at which the SR tests were performed is shown in Fig. 5. Open circles and full circles depict the internal stress σ_i, and the effective stress σ^*, respectively. It is obvious that the internal stress σ_i is a substantial contribution to the applied stress σ_{ap}. Similar curves estimated at 150 °C are shown in Fig. 6. The effective stress component increases with increasing strain while the internal stress increases to the maximum and then decreases with increasing strain. Fig. 7 shows the curves obtained at 300 °C. The internal stress is lower than the effective stress and it decreases for strains higher than $\varepsilon = 0.02$. The internal stress depends on the dislocation density, i.e. $\sigma_i \propto \rho^{1/2}$. A decrease of the internal stress indicates a decrease of the dislocation density. In the case when the internal stress is approximately constant or slightly decreasing with strain, some equilibrium between multiplication and annihilation of dislocations may be considered.

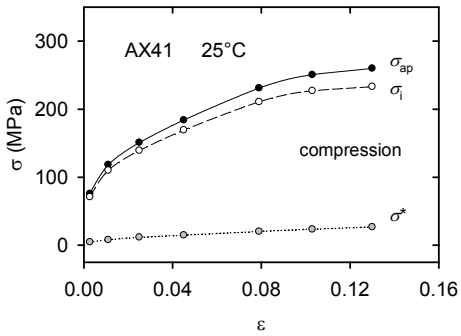

Fig. 5. A part of the true stress–true strain curve obtained for the AX41 alloy at 25 °C in compression. The points of σ_{ap} on the curve indicate the stresses at which the SR tests were performed.

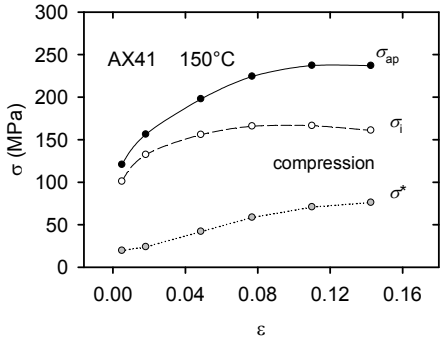

Fig. 6. A part of the true stress-true strain curve obtained for the AX41 alloy at 150 °C in compression. The points of σ_{ap} on the curve indicate the stresses at which the SR tests were performed.

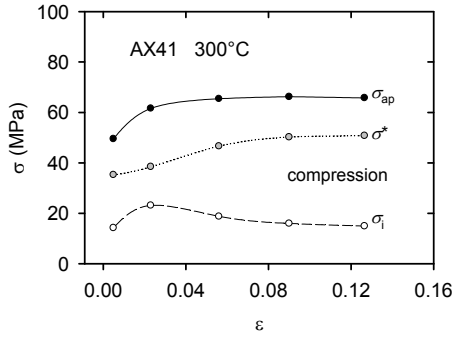

Fig. 7. Part of the stress– strain curve for AX41 alloy at 300 °C. The points of σ_{ap} on the curve indicate the stresses at which the SR tests were performed.

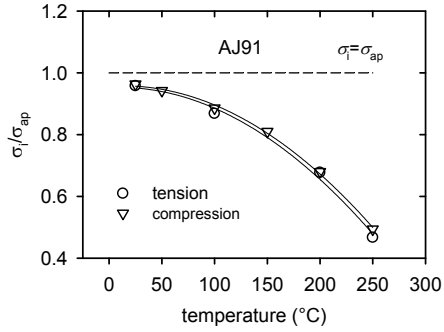

Fig. 8. Variation of the internal/applied stress ratio obtained from the first SR test with temperature estimated for the AJ91 samples.

The moving dislocations can cross slip and after cross slip they may annihilate, which causes the decrease in the dislocation density. At higher temperatures, the moving dislocations can also climb. The activity of cross slip and climb increases with increasing temperature. This means that the total dislocation density decreases with increasing temperature. The internal stress/applied stress ratio decreases significantly with increasing temperature independent of the deformation mode (the values of the ratio for compression deformation are practically the same as for tension) (see Fig. 8 where the temperature dependence of σ_i/σ_{ap} is introduced for AJ91 alloy). It is possible to estimate the internal stress also in creep experiments as it was performed by Milička et al. (Milička et al., 2007) for several magnesium alloys. They found that the internal stress σ_i reflects the creep resistance of the material. Experimental internal stresses determined in creep well correspond to those determined in SR tests under comparable testing conditions.

5. Thermally activated dislocation motion

The deformation behaviour of materials depends on temperature and strain rate. Practically in all polycrystals, the temperature and strain rate dependences of the flow stresses can be found. These dependences indicate thermally activated processes. The motion of dislocations through a crystal is affected by many kinds of obstacles. The mean velocity of dislocations is connected with the strain rate by the Orowan equation

$$\dot{\varepsilon} = (1/M)\rho_m b v \tag{21}$$

where ρ_m is the density of mobile dislocations moving at a mean velocity v. It is obvious that the stress dependence of $\dot{\varepsilon}$ is done by the stress dependence of ρ and v. At a finite temperature, the obstacles can be overcome with the help of thermal fluctuations. Therefore, the dislocations are able to move even if the force on dislocations is lower than that exerted by the obstacles; the additional energy is supplied by thermal fluctuations. The short-range thermally activated processes are important for the understanding of deformation behaviour. If a single process is controlling the rate of dislocation glide, the plastic strain rate $\dot{\varepsilon}$ can be expressed as:

$$\dot{\varepsilon} = \dot{\varepsilon}_0 \exp\left[-\frac{\Delta G(\sigma^*)}{k_B T}\right], \tag{22}$$

where $\dot{\varepsilon}_0$ is a pre-exponential factor containing the mobile dislocation density, the average area covered by the dislocations in every activation act, the Burgers vector, the vibration frequency of the average dislocation segment and a geometric factor. $\Delta G(\sigma^*)$ is the change in the Gibbs free enthalpy depending on the effective stress $\sigma^*=\sigma-\sigma_i$, T is the absolute temperature and k_B is the Boltzmann constant. The stress dependence of the free enthalpy may be expressed by a simple relation

$$\Delta G(\sigma^*) = \Delta G_0 - V\sigma^* = \Delta G_0 - V(\sigma - \sigma_i), \tag{23}$$

where ΔG_0 is the Gibbs free enthalpy necessary for overcoming a short-range obstacle without the stress and V = bdL is the activation volume where d is the obstacle width and L is the mean length of dislocation segments between obstacles. It should be mentioned that L may depend on the stress acting on dislocation segments.

The nature and the distribution of obstacles determine the activation parameters (the activation energy and the activation volume). For a given arrangement of obstacles in a material, the thermally activated process controls the temperature and strain rate dependence of the flow stress. Two methods are very often used for the estimation of the activation volume: differential constant strain rate tests and stress relaxation experiments. In differential constant strain rate tests, the specimen is deformed with a constant strain rate to a given strain (stress) and then the strain rate is suddenly changed by a known factor. The resulting change in stress is observed; an increase (decrease) in the stress is observed if the strain rate increases (decreases). The activation volume is inversely proportional to this stress change. The activation volume can be estimated from the stress relaxation tests. The stress decrease with time during the SR test can be described by the known Feltham equation (Feltham, 1963)

$$\Delta\sigma(t) = \sigma(0) - \sigma(t) = \alpha\ln(\beta t + 1)\,, \tag{24}$$

where $\sigma(0)$ is the stress at the beginning of the stress relaxation at time $t = 0$, β is a constant. The activation volume is done by:

$$\alpha = \frac{k_B T}{V}\,. \tag{25}$$

and the constant β

$$\beta = \frac{M\dot{\varepsilon}_0 V}{k_B T}\exp\left[-\frac{\Delta G_0 - V\sigma^*(0)}{k_B T}\right] = \frac{M\dot{\varepsilon}(0)}{\alpha}\,. \tag{26}$$

Values of the apparent activation volume estimated using Eq. (24) are plotted against the applied stress in Fig. 9 for AJ51 and in Fig. 10 for AZ63 alloys for several deformation temperatures. The activation volume depends on the applied stress and testing temperature. Apparent (experimental) activation volume estimated in experiments with polycrystals is proportional to the dislocation activation volume, $V_{d,}$ as $V = (1/M)V_d$. Usually, the values of activation volume are given in b^3, which allows their comparison with processes responsible for the thermally activated dislocation motion. Apparent activation volumes for AJ51 alloy estimated for four deformation temperatures in tensile (T) and compression (C) tests are plotted against the effective (thermal) stress in Fig. 11. All values appear to lie on one line, "master curve". Similar results were found for other magnesium alloys among them also for AZ63 alloy (see Fig. 12).

In order to analyse the dependences, we will assume an empirical relation between the Gibbs free enthalpy Δ G and the effective stress, σ^*, suggested by Kocks and co-workers (Kocks et al., 1975) in the following form:

$$\Delta G = \Delta G_0\left[1 - \left(\frac{\sigma^*}{\sigma_0^*}\right)^p\right]^q \tag{27}$$

where σ_0^* is the effective stress at 0 K. From (22) and (27) it follows:

$$\sigma^* = \sigma_0^*\left[1 - \left(\frac{k_B T}{\Delta G_0}\ln\frac{\dot{\varepsilon}_0}{\dot{\varepsilon}}\right)^{1/q}\right]^{1/p}\,, \tag{28}$$

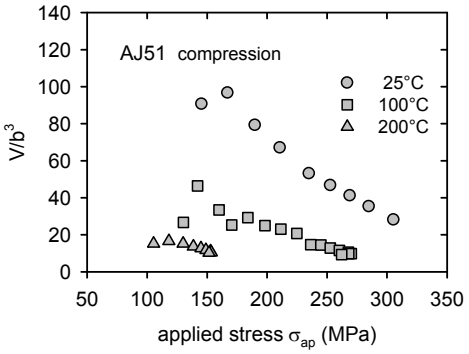

Fig. 9. Plot of the apparent activation volume (in b^3) against the applied stress σ_{ap} estimated for the AJ51 alloy in compression, at three temperatures.

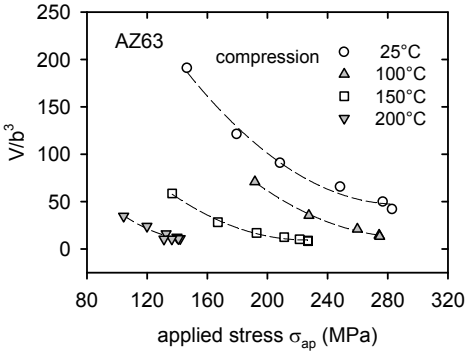

Fig. 10. Plot of the apparent activation volume (in b^3) against the applied stress σ_{ap} estimated for four deformation temperatures in compression.

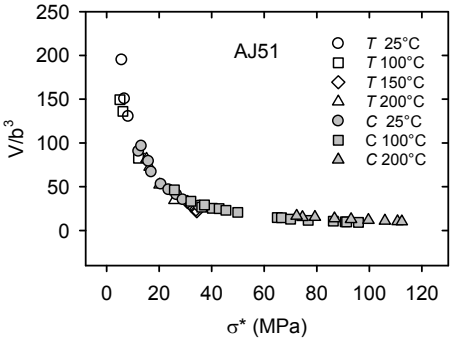

Fig. 11. Plot of the apparent activation volume (in b^3) against the thermal stress σ^* estimated for four deformation temperatures in tension (T) and compression (C) for the AJ51 alloy.

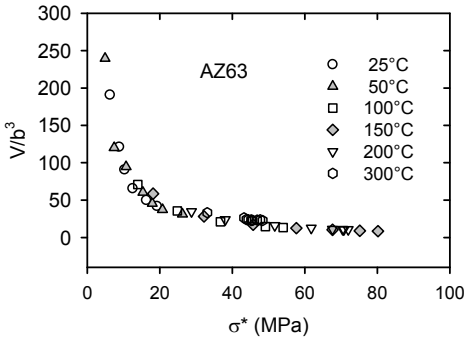

Fig. 12. Plot of the apparent activation volume (in b^3) against the thermal stress σ^* estimated for various deformation temperatures (AZ63 alloy).

where p and q in Eqs. (27) and (28) are phenomenological parameters reflecting the shape of a obstacle profile. The possible ranges of values p and q are limited by the conditions $0 < p \leq 1$ and $1 \leq q \leq 2$. Ono (Ono, 1968) and Kappor and co-workers (Kapoor et al., 2002) suggested that Eq. (28) with $p = 1/2$, $q = 3/2$ describes a barrier shape profile that fits many predicted barrier shapes. Equation (28) can be rewritten as

$$\dot{\varepsilon} = \dot{\varepsilon}_0 \exp\left[-\frac{\Delta G_0}{k_B T} \left(1 - \left(\frac{\sigma^*}{\sigma_0^*} \right)^p \right)^q \right]. \tag{29}$$

The dependence of the activation volume on the effective stress can be expressed as

$$V = k_B T \frac{\partial \ln \dot{\varepsilon} / \dot{\varepsilon}_0}{\partial \sigma^*} = \frac{\Delta G_0 pq}{\sigma_0^*} \left[1 - \left(\frac{\sigma^*}{\sigma_0^*} \right)^p \right]^{q-1} \left(\frac{\sigma^*}{\sigma_0^*} \right)^{p-1} . \quad (30)$$

The values of the activation volume should lie at the curve given by Eq. (30). The fit of the experimental values of Eq. (30) gives for the activation enthalpy ΔG_0 = 0.95 ± 0.05 eV for both alloys (AJ51 and AZ63). Similar values ΔG_0 ~ 1.00 ± 0.05 eV were estimated for all magnesium alloys studied. The values of the activation volume and the activation enthalpy may help to identify thermally activated process considering some of the common short range barriers to dislocation motion. We should consider that a rapid decrease in the internal stress with increasing temperature indicates that observed softening during deformation is connected with dynamic recovery. It is well-known that the main deformation mode in magnesium and magnesium alloys with hcp structure is basal glide system with dislocations of the Burgers vector <a> = $1/3[11\bar{2}0]$. The secondary conservative slip may be realised by the <a> dislocations on prismatic and pyramidal of the first-order. Couret and Caillard (Couret and Caillard, 1985a,b) using TEM showed that the screw dislocations with the Burgers vector of $1/3[11\bar{2}0]$ in magnesium are able to glide on prismatic planes and their mobility is much lower than the mobility of edge dislocations. They concluded that the deformation behaviour of magnesium over a wide temperature range is controlled by thermally activated glide of those screw dislocation segments. A single controlling mechanism has been identified as the Friedel-Escaig cross slip mechanism. This mechanism assumes dissociated dislocations on compact planes, like (0001), that joint together along a critical length L_{cr} producing double kinks on non-compact planes. Therefore, the activation volume is proportional to the critical length between two kinks. The activation volume of the Friedel–Escaig mechanism has a value of ~70 b^3. Prismatic slip has been also observed by Koike and Ohyama (Koike & Ohyama, 2005) in deformed AZ61 sheets. The activation of the prismatic slip and subsequent annihilation of the dislocation segments with the opposite sign are probably the main reason for the observed internal stress decrease. The double cross slip may be thermally activated process controlling the dislocation velocity. The activation of the prismatic slip of <a> dislocations and subsequent annihilation of the dislocation segments with the opposite sign may contribute to the observed internal stress decrease.

The number of independent slip systems in the basal plane is only two. Thus, the von Mises requirement for five independent deformation modes to ensure a reasonably deformability of magnesium alloy polycrystals is not fulfilled. Twinning and the activity of non-basal slip is required. From activities of non-basal slip systems, motion of dislocations with <c+a> Burgers vector in the second-order pyramidal slip systems is expected. The critical resolved shear stress (CRSS) for non-basal slip systems at room temperature is higher by about a factor 100 than the CRSS for basal slip. On the other hand, the CRSS for non-basal slip decreases rapidly with increasing temperature. It means that the activity of a non-basal slip system increases with increasing temperature. It is worth mentioning that Máthis and co-workers (Máthis et al., 2004b), who studied the evolution of different types of dislocations with temperature in Mg using X-ray diffraction, found that at higher temperatures, the fraction of <c+a> dislocations increases at a cost of <a> dislocations. The total dislocation density decreases with increasing temperature. The glide of <c+a> dislocations may affect the deformation behaviour of magnesium alloys.

The shape of the true stress – true strain curves (Figs. 1-3) indicates that the flow stress and strain hardening and softening are influenced by the testing temperature – at temperatures above about 200 °C, the strain hardening is very close to zero. From the dislocation theory point of view, this deformation behaviour may be explained assuming changes in deformation mechanisms. At temperatures below about 200 °C, strain hardening is caused by multiplication and storage of dislocations. Above about 200 °C, there is not only storage of dislocations during straining leading to hardening but also annihilation of dislocations leading to softening. The intensity of the latter is highly dependent on temperature. A dynamic balance between hardening and softening may take place at higher temperatures. The activity of non-basal slip systems has to play an important role in both hardening and recovery processes in magnesium alloys. The glide of <c+a> dislocations may be responsible for an additional work hardening because of the development of several systems of immobile or sessile dislocations. Different reactions between <a> basal dislocations and <c+a> pyramidal dislocations can occur (Lukáč, 1981; Lukáč, 1985). Glissile (glide) <c+a> dislocations can interact with <a> dislocations – immobile <c> dislocations may arise within the basal plane according to the following reaction:

$$\tfrac{1}{3}\left\langle 2\bar{1}\bar{1}3\right\rangle + \tfrac{1}{3}\left\langle \bar{2}110\right\rangle \rightarrow \left\langle 0001\right\rangle \ . \tag{31}$$

Another reaction that employs the basal <a> dislocations yields a sessile <c+a> dislocation

$$\tfrac{1}{3}\left\langle 2\bar{1}\bar{1}3\right\rangle + \tfrac{1}{3}\left\langle \bar{1}2\bar{1}0\right\rangle \rightarrow \tfrac{1}{3}\left\langle 11\bar{2}3\right\rangle \ . \tag{32}$$

Finally, a combination of two glissile <c+a> dislocations gives rise to a sessile dislocation of <a> type that lays along the intersection of the second order pyramidal planes according to the following reaction:

$$\tfrac{1}{3}\left\langle 2\bar{1}\bar{1}3\right\rangle + \tfrac{1}{3}\left\langle \bar{1}2\bar{1}\bar{3}\right\rangle \rightarrow \tfrac{1}{3}\left\langle 11\bar{2}0\right\rangle . \tag{33}$$

Different dislocation reactions may produce both sessile and glissile dislocations. Production of sessile dislocations increases the density of the forest dislocations that are obstacles for moving dislocations. Therefore, an increase in the flow stress with straining follows, which is observed in the experiment. On the other hand, screw components of <c+a> (and also <a>) dislocation may move to the parallel slip planes by double cross slip and they can annihilate – the dislocation density decreases, which leads to softening. One has to consider that twins and grain boundaries are also obstacles for moving dislocations in polycrystalline materials. Dislocation pile-ups are formed at the grain boundaries. The stress concentrations at the head of pile-ups contribute to initiations of the activity of the pyramidal slip systems. Another possible source mechanism for <c+a> dislocations was proposed by Yoo and co-workers (Yoo et al., 2001). The scenario described above can help in understanding the deformation behaviour of magnesium alloy over a wide temperature range. The increase in the elongation to failure with increasing temperature can be also explained by an increase in the activity of non-basal slip systems. At certain, sufficient, level of the flow stress, the non-basal slip becomes active. To describe the evolution of dislocations in both slip systems, it is necessary to take into account the storage and annihilation in both slip systems (basal and non-basal) and mutual interaction.

Very recently, it has been reported atomistic study of edge and screw <c+a> dislocations in magnesium (Nogaret et al. 2010). They concluded that at 300 K both screw and edge <c+a> dislocations may glide at stresses smaller than the experimentally observed.

6. Strain ageing

From the temperature dependence of the yield stress, introduced in Fig. 13 for AZ63 alloy, some local maximum between 50 and 100 °C is obvious. This maximum is a consequence of dynamic strain ageing. It is also manifested at the stress strain curve by the so called post relaxation effect. When the internal stress as well as the dislocation density are constant then the deformation process continues at the same stress as at the beginning of the SR test. On the stress - strain curve shown in Fig. 14, a stress increase after SR test is obvious. The flow stress after the stress relaxation, σ_1, is higher than the flow stress at the beginning of the relaxation. The values of $\Delta\sigma = \sigma_1 - \sigma_0$ are plotted against strain for two temperatures of 25 and 50 °C in Fig. 15. For other temperatures the post relaxation effect was not observed. From Fig. 15 it can be seen that the strain dependence of $\Delta\sigma$ has some maximum at a certain strain. Analogous maximum was found in the stress dependence of the stress increment. Similar results were found for alloys containing the rare earth in the temperature interval between 150 and 250 °C (Fig. 16) (Trojanová et al., 2005), while such effects may be observed in alloys of the AZ series slightly over room temperature (Trojanová et al., 2001).

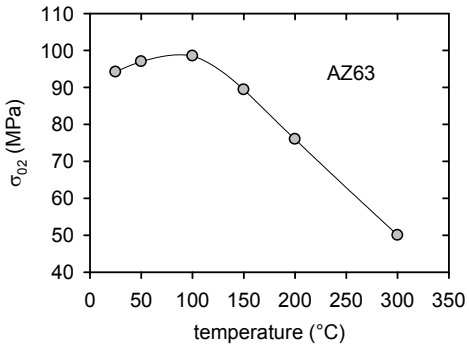

Fig. 13. Temperature dependence of the yield stress obtained for AZ63 alloy.

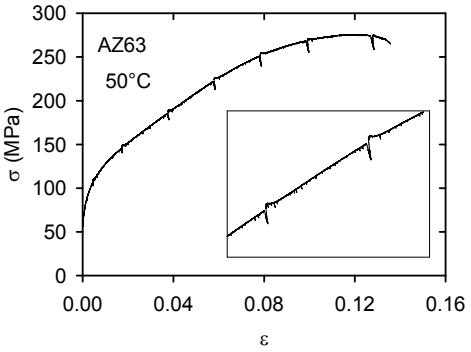

Fig. 14. The stress-strain curve obtained at 50 °C. An increase of the stress after the stress relaxation test is from the insert well visible (AZ63 alloy).

In an alloy the flow stress may be consider as a sum of two additive contributions:

$$\sigma = \sigma_f + \sigma_d \,, \tag{34}$$

with σ_f relating to a friction imposed by the solutes-dislocation interaction, σ_d relating to the dislocation–dislocation interaction. Hong (Hong, 1987, 1989) suggested that the stress σ_f could be described by the following equation:

$$\sigma_f = \alpha_1 G b \delta c \exp\left(-\frac{(T-T_0)^2}{B}\right), \tag{35}$$

where α_1 is a constant, δ is the atomic size misfit parameter, c is the solute concentration and B is the width of the distribution about the temperature T_0 where the maximum of solute-dislocation interaction force occurs. The critical dislocation velocity V_c at which the maximum force occurs can be expressed as:

$$V_c = \alpha_2 \frac{kT_0 D_0}{Gb\delta\Omega} \exp\left(-\frac{Q_D}{k_B T}\right), \tag{36}$$

where α_2 is a constant, D_0 is the diffusion constant for solute atoms, Ω is the atomic volume and Q_D is the activation energy for diffusion of solute atoms in magnesium matrix. The critical strain rate at which the maximum interaction stress occurs can be predicted using the following equation:

$$\dot{\varepsilon}_c = \rho_m b \frac{\pi(1-\nu)kT_0 D_0}{(1+\nu)Gb\delta\Omega} \exp\left(-\frac{Q_D}{k_B T}\right), \tag{37}$$

where ν is the Poisson ratio, ρ_m is the mobile dislocation density. From Eq. (35) it can be seen that the friction force due to solute atoms interaction with moving dislocations exists only in a certain temperature interval depending on solute atoms type. This friction force (stress) is added to the temperature dependence of the yield stress resulting to a local maximum in the temperature dependence of the yield stress. Such local maximum in the temperature dependence is demonstrated in Fig. 15 for AZ63 alloy and in Fig. 16 for the binary Mg-Nd alloy at 150 and 200 °C (Trojanová & Lukáč, 2010). Similar local maximum was observed in the case of ZE41 alloy (Trojanová & Lukáč, 2005), AZ91 alloy (Trojanová et al., 2001).

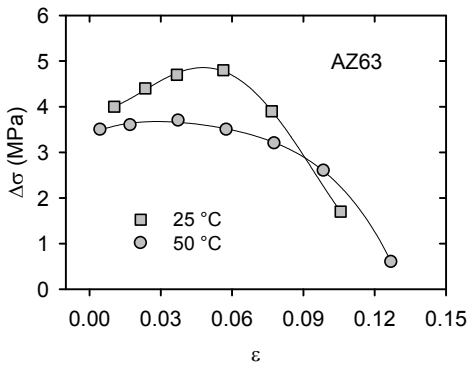

Fig. 15. The stress increase $\Delta\sigma$ depending on the strain estimated for AZ63 alloy at 25 and 50 °C.

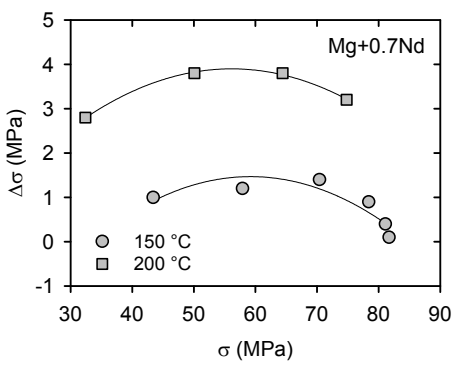

Fig. 16. The stress increase $\Delta\sigma$ depending on the stress estimated for Mg-0.7%Nd at 150 and 200 °C.

According to Malygin (Malygin, 1986) and Rubiolo and Bozzano (Rubiolo & Bozzano, 1995) solute atoms diffuse to dislocations arrested at local obstacles for waiting time t_w. The concentration of solute atoms at dislocation lines as a function of the waiting time $c(t_w)$ is done by the following function

$$c = c_m \left[1 - \exp\left(-\frac{c_0}{c_m} \left(\alpha_n D t_w / b^2 \right) \right)^{2/(n+2)} \right], \tag{38}$$

where

$$\alpha_n = n(n+2)\pi^{(n+2)/2} \left(W_B / k_B T \right). \tag{39}$$

c_0 is the average concentration of impurities in the crystal and c_m is the limiting value of impurities on the dislocations. W_B is the binding energy of solute atoms to dislocations. The value of n depends on the details of interaction between solute atom and dislocations. The exponent in Eq. (38) $p=2/(n + 2)$ is typically 2/3 and 1/3 for bulk and pipe diffusion, respectively (Balík & Lukáč, 1998). The stress increment $\Delta\sigma$ after SR due to solute atoms segregation may be also expressed for longer time by the following equation

$$\Delta\sigma(t,\varepsilon,T) = \Delta\sigma_m(\varepsilon,T) \{1 - \exp[-(t/t_c)']\}, \tag{40}$$

where $\Delta\sigma_m(\varepsilon,T)$ is the stress increment for $t\to\infty$ and it depends on the binding energy between solute atoms and dislocations. (It increases with increasing solute atom concentration and with decreasing temperature.) t_c is a characteristic time which depends on the strain as $t_c \sim \varepsilon^{-k}$. (Lubenets et al., 1986). Solute atoms locking dislocations cause the stress increase after stress relaxation, which depends on strain and on temperature. An increase in the flow stress is needed to move the dislocations after stress relaxation. It is reasonably to assume that $\Delta\sigma$ is proportional to the number of impurities on dislocation lines.

Concluding remarks

It should be noted that it is generally accepted that twinning plays an important role during plastic deformation of magnesium alloys. Twins influence also ductility in different way depending on the tensile/compression tests (Barnett, 2007a; 2007b). The effect of twins depends on the testing temperature and strain (Barnett at al., 2005). Serra and Bacon (Serra and Bacon, 2005) concluded that the motion of the twinning dislocations is thermally activated. The mobility of such dislocations increases with increasing temperature.

7. Acknowledgements

The authors dedicate this paper to Prof. RNDr. František Chmelík, CSc., on the occasion of his 50th birthday. This work received a support from the Ministry of Education, Youth and Sports of the Czech Republic by the project MSM 0021620834. This work was also supported by the Grant Agency of the Academy of Sciences of the Czech Republic under Grant IAA201120902.

8. References

Akthar, A. & Teghtsoonian, E. (1972). Substitutional solution hardening of magnesium single crystals. *Phil. Mag.*, *25*, 897-905, ISSN: 1478-6435.

Balík, J. & Lukáč, P. (1998). On the kinetics of dynamic strain ageing. *Kovove Mater.*, 36, 3-9, . ISSN: 0023-432X.

Balik, J.; Lukáč, P.; Drozd, Z. & Kužel, R. (2009). Strain hardening of AZ31 magnesium alloy. *Int. J. Mat. Res.*, 100, 322-325, ISSN: 1862-5282.

Barnett, M.R.; Davies, C.H.J. & Ma, X. (2005). An analytical constitutive law for twinning dominated flow in magnesium. Scripta Mater. 52, 627-632, ISSN: 1359-6462.

Barnett, M.R. (2007a). Twinning and the ductility of magnesium alloys. Part I: "Tension" twins. *Mater. Sci. Eng. A*, 464, 1-7, ISSN: 0921-5093.

Barnett, M.R. (2007b). Twinning and the ductility of magnesium alloys. Part II: "Contraction" twins. *Mater. Sci. Eng. A*, 464, 8-16, ISSN: 0921-5093.

Braasch, H.; Estrin, Y. & Brechet, Y. (1996). A stochastic model for dislocation density evolution. *Scripta Mater.*, 35, 279-284, ISSN: 1359-6462.

Cáceres, C.H. & Lukáč, P. (2008). Strain hardening behaviour and the Taylor factor of pure magnesium. *Phil. Mag.*, 88, 977-989, ISSN: 1478-6435.

Couret, A. & Caillard, D. (1985a). An *in situ* study of prismatic glide in magnesium – I. The rate controlling mechanism. *Acta metall.*, 33, 1447–1454, ISSN: 1359-6454.

Couret, A. & Caillard, D. (1985b). An *in situ* study of prismatic glide in magnesium – II. Microscopic activation parameters. *Acta metall.*, 33, 1455–1462, ISSN: 1359-6454.

Estrin, Y. & Mecking, H. (1984). A unified phenomenological decription of work hardening and creep based on one-parameter models. *Acta Metall.*, 32, 57-70, ISSN: 1359-6454.

Estrin, Y. & Kubin, L. (1986). Local strain hardening and nonuniformity of plastic deformation. *Acta Metall.*, 34, 2455-2464. ISSN: 1359-6454.

Estrin, Y. (1996). Dislocation-density-related constitutive modelling. In: *Unified constitutive laws of plastic deformation*. Krausz, A.S. & Krausz, K. (Eds.), 69-105, Academic Press, ISBN: 0-12-425970-7, New York.

Feltham, P. (1963). Stress relaxation in magnesium at low temperatures. *Phys. Stat. Sol.*, 3. 1340–1346, ISSN: 1862-6300.

Hong, S. I. (1987). Influence of dynamic strain aging on the creep ductility of solid solution alloys. *Mater. Sci. Eng.*, 91, 137-142, ISSN: 0921-5093.

Hong, S. I. (1989). Influence of dynamic strain aging on the transition of creep characteristics of a solid solution alloy at various temperatures. *Mater. Sci. Eng. A,* 110, 125-130, ISSN: 0921-5093.

Kapoor, R.; Wadekar, S.L. & Chakravartty, J.K. (2002). Deformation in Zr-1Nb-1Sn-0.1Fe using stress relaxation technique. *Mater. Sci. Eng. A,* 328, 324–333, ISSN: 0921-5093.

Kocks, U.F. (1976). Laws for work hardening and low-temperature creep. *J. Eng. Mater.Techn.*, 98, 76-85, ISSN (printed): 0094-4289. ISSN (electronic): 1528-8889.

Kocks, U.F.; Argon, A.S. & Ashby, M.F. (1975). Thermodynamics and kinetics of slip. *Progr. Mater. Sci.*, 19, 1–288, ISSN: 0079-6425.

Koike, J. & Ohyama, R. Mater., 53, 1963. Geometrical criterion for the activation of prismatic slip in AZ61 Mg alloy sheets deformed at room temperature. *Acta Mater.*, 53 (2005) 1963–1972, ISSN: 1359-6454.

Li, J.C.M, (1967). Dislocation dynamics in deformation and recovery *Canad. J. Appl. Phys.*, 45 493–509. ISSN : 0008-4204..

Li, J.C.M. (1981). On stress relaxation based on dislocation dynamics. *Scripta Metall.*, 15, 935-936, ISSN: 1359-6462.

Lubenets, S.V.; Startsev, V.I. & Fomenko, L.S. (1986). Strain aging kinetics in indium-based alloys. *Czech. J. Phys. B*, 36, 493-497, ISSN: 0011-4626.

Lukáč, P. (1981). Plastic deformation of hexagonal metals. *Czech. J. Phys. B*, 31, 135-141, ISSN: 0011-4626.

Lukáč P. (1985). Hardening and softening during plastic deformation of hexagonal metals. *Czech. J. Phys. B*, 35, 275-285, ISSN: 0011-4626.

Lukáč, P. & Balík, J. (1994). Kinetics of plastic deformation. *Key Engn. Mater*., 97-98, 307-322, ISBN: 0-87849-687-4

Malygin, G.A. (1990). Dislocation density evolution equation and strain hardening of f.c.c. crystals. *Phys. Stat. Sol. (a)*. 119, 423-436, ISSN: 1862-6300.

Malygin, G.A. (1982). Impurity atmospheres and effective activation parameters of dislocation motion with special reference to Al-Mg and Zr-O alloys. *Phys. Stat. Sol. (a)*, 1982, 72, 493-501, ISSN: 1862-6300.

Máthis, K.; Trojanová, Z.; Lukáč, P.; Cáceres, C.H. & Lendvai, J. 2004a). Modeling of hardening and softening processes in Mg alloys. *J. Alloys Comp*., 378, 176-179, ISSN**:** 0925-8388.

Máthis, K.; Nyilas, K.; Axt, A.; Dragomir-Cernatescu, I.; Ungár, T. & Lukáč, P. (2004b). The evolution of non-basal dislocations as a function of deformation temperature in pure magnesium determined by X-ray diffraction. *Acta Mater*., 52, 2889–2894, ISSN: 1359-6454.

Máthis, K. & Trojanová, Z. (2005). Application of Lukáč-Balík model for characterization of work hardening behaviour of Mg-Zn and Mg-Al alloys. *Kovové Mater.* 43, 238-244, ISSN: 0023-432X.

Milička, K.; Trojanová, Z. & Lukáč, P. (2007). Internal stresses during creep of magnesium alloys at 523 K. *Mater. Sci. Eng. A*, 462, 215–219, ISSN: 0921-5093.

Nes, E. & Marthinsen, K. (2002). Modeling the evolution in microstructure and properties during plastic deformation of fcc-metals and alloys –an approach towards a unified model. *Mater. Sci. Eng. A*, 322, 176-193, ISSN: 0921-5093.

Nogaret, T.;Curtin, W.A.;Yasi, J.A.; Hector Jr, L.G. & Trinkle, D.R. (2010). Atomistic study of edge and screw <c+a> dislocations in magnesium. *Acta Mater*., 58, 4332-4343, ISSN: 1359-6454.

Ono, K. (1968). Temperature dependence of dispersed barrier hardening. *J. Appl. Phys*., 39, 1803–1806, ISSN: 0021-8979.

Rubiolo, G.H. & Bozzano, P.B (1995). Dynamic interaction of impurity atmospheres with moving dislocations during stress relaxation. *Mater. Trans. JIM*, 36, 1124-1133, ISSN: 1345-9678.

Serra, A. & Bacon, D.J. (2005). Modelling the motion of $\{11\bar{2}2\}$ twinning dislocations in the hcp metals. *Mater. Sci. Eng. A*, 400-401, 496-498, ISSN: 0921-5093.

Trojanová, Z.; Lukáč, P.; Gabor, P.; Drozd, Z. & Máthis, K. (2001). Stress relaxation in an AZ91 magnesium alloy. *Kovove Mater*., 39, 368-378, ISSN: 0023-432X.

Trojanová, Z.; Lukáč, P.; Kainer, K.U. & Gärtnerová, V. (2005). Dynamic strain ageing in selected magnesium alloys containing rare earth elements. *Adv. Engn. Mater*., 7, 1027-1032, ISSN: 1438-1656.

Trojanová, Z. & Lukáč, P. (2005). Compressive deformation of ZE41 magnesium alloy between 23 and 300 ^{o}C. *Kovove Mater*., 43, 73-80, ISSN: 0023-432X.

Trojanová. Z. & Lukáč, P. (2010). Mobility of solute atoms in a Mg-Nd alloy studies by nondestructive and destructive methods. In: *Magnesium Alloys and their Applications 8*, Kainer, K.U. (Ed), 785-802, Willey-VCH, ISBN: 978-3-527-32732-4, Weinheim.

Yoo, M.H.; Agnew, S.R.; Morris, J.R. & Ho, K. (2001). Non-basal slip systems in hcp metals and alloys: source mechanisms. *Mater. Sci. Eng.* A, 321, p. 87-92. ISSN: 0921-5093.

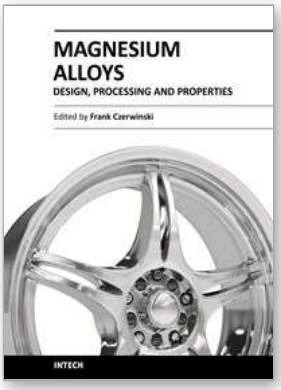

Magnesium Alloys - Design, Processing and Properties

Edited by Frank Czerwinski

ISBN 978-953-307-520-4
Hard cover, 526 pages
Publisher InTech
Published online 14, January, 2011
Published in print edition January, 2011

Scientists and engineers for decades searched to utilize magnesium, known of its low density, for light-weighting in many industrial sectors. This book provides a broad review of recent global developments in theory and practice of modern magnesium alloys. It covers fundamental aspects of alloy strengthening, recrystallization, details of microstructure and a unique role of grain refinement. The theory is linked with elements of alloy design and specific properties, including fatigue and creep resistance. Also technologies of alloy formation and processing, such as sheet rolling, semi-solid forming, welding and joining are considered. An opportunity of creation the metal matrix composite based on magnesium matrix is described along with carbon nanotubes as an effective reinforcement. A mixture of science and technology makes this book very useful for professionals from academia and industry.

How to reference

In order to correctly reference this scholarly work, feel free to copy and paste the following:

Zuzanka Trojanova and Pavel Lukac (2011). Hardening and Softening in Magnesium Alloys, Magnesium Alloys - Design, Processing and Properties, Frank Czerwinski (Ed.), ISBN: 978-953-307-520-4, InTech, Available from: http://www.intechopen.com/books/magnesium-alloys-design-processing-and-properties/hardening-and-softening-in-magnesium-alloys

INTECH
open science | open minds

InTech Europe
University Campus STeP Ri
Slavka Krautzeka 83/A
51000 Rijeka, Croatia
Phone: +385 (51) 770 447
Fax: +385 (51) 686 166
www.intechopen.com

InTech China
Unit 405, Office Block, Hotel Equatorial Shanghai
No.65, Yan An Road (West), Shanghai, 200040, China
中国上海市延安西路65号上海国际贵都大饭店办公楼405单元
Phone: +86-21-62489820
Fax: +86-21-62489821